INTERFACE

rsif.royalsocietypublishing.org

Research

Cite this article: Cui X *et al*. 2017 Enhanced osteointegration of poly(methylmethacrylate) bone cements by incorporating strontium-containing borate bioactive glass. *J. R. Soc. Interface* **14**: 20161057.
http://dx.doi.org/10.1098/rsif.2016.1057

Received: 8 February 2017
Accepted: 23 May 2017

Subject Category:
Life Sciences–Chemistry interface

Subject Areas:
biomaterials

Keywords:
poly(methylmethacrylate) cement, strontium-containing borate bioactive glass, biocompatibility, osseointegration

Authors for correspondence:
Changshun Ruan
e-mail: cs.ruan@siat.ac.cn
Haobo Pan
e-mail: hb.pan@siat.ac.cn

Enhanced osteointegration of poly(methylmethacrylate) bone cements by incorporating strontium-containing borate bioactive glass

Xu Cui[1], Chengcheng Huang[1], Meng Zhang[1], Changshun Ruan[1], Songlin Peng[2], Li Li[3], Wenlong Liu[1], Ting Wang[4], Bing Li[3], Wenhai Huang[5], Mohamed N. Rahaman[6], William W. Lu[1,7] and Haobo Pan[1]

[1]Center for Human Tissues and Organs Degeneration, Shenzhen Institute of Advanced Technology, Chinese Academy of Sciences, Shenzhen 518055, People's Republic of China
[2]Department of Spine Surgery, Shenzhen People's Hospital, Jinan University School of Medicine, Shenzhen 518020, People's Republic of China
[3]The Fourth Affiliated Hospital of Guangxi Medical University/Liu Zhou Worker's Hospital, Liuzhou 545005, People's Republic of China
[4]Shenzhen Key Laboratory for Innovative Technology in Orthopaedic Trauma, Department of Orthopaedics, The University of Hong Kong-Shenzhen Hospital, University of Hong Kong, Shenzhen, People's Republic of China
[5]Institute of Bioengineering and Information Technology Materials, Tongji University, Shanghai 200092, People's Republic of China
[6]Department of Materials Science and Engineering, Center for Biomedical Science and Engineering, Missouri University of Science and Technology, Rolla, MO 65409-0340, USA
[7]Department of Orthopaedics and Traumatology, The University of Hong Kong, Room 907, Lab Block, 21 Sassoon Road, Hong Kong SAR, People's Republic of China

XC, 0000-0003-1235-7982

Although poly(methylmethacrylate) (PMMA) cements are widely used in orthopaedics, they have numerous drawbacks. This study aimed to improve their bioactivity and osseointegration by incorporating strontium-containing borate bioactive glass (SrBG) as the reinforcement phase and bioactive filler of PMMA cement. The prepared SrBG/PMMA composite cements showed significantly decreased polymerization temperature when compared with PMMA and retained properties of appropriate setting time and high mechanical strength. The bioactivity of SrBG/PMMA composite cements was confirmed *in vitro*, evidenced by ion release (Ca, P, B and Sr) from SrBG particles. The cellular responses of MC3T3-E1 cells *in vitro* demonstrated that SrBG incorporation could promote adhesion, migration, proliferation and collagen secretion of cells. Furthermore, our *in vivo* investigation revealed that SrBG/PMMA composite cements presented better osseointegration than PMMA bone cement. SrBG in the composite cement could stimulate new-bone formation around the interface between the composite cement and host bone at eight and 12 weeks post-implantation, whereas PMMA bone cement only stimulated development of an intervening connective tissue layer. Consequently, the SrBG/PMMA composite cement may be a better alternative to PMMA cement in clinical applications and has promising orthopaedic applications by minimal invasive surgery.

1. Introduction

Since the 1960s [1], poly(methylmethacrylate) (PMMA) bone cement has been widely used in orthopaedics, especially for kyphoplasty, vertebroplasty and arthroplasty [2,3], owing to its desirable mechanical strength, relatively low toxicity and good handleability in the surgical process [4]. However, due to the lack of osseointegration, PMMA bone cement cannot bond directly to bone but forms an intervening connective tissue layer between the bone and

THE ROYAL SOCIETY PUBLISHING

cement, which occasionally leads to aseptic loosening of the prostheses when used for arthroplasty [5]. In addition, the peak polymerization temperature of PMMA may increase up to 100°C due to heat release during the polymerization process of MMA monomers, which compromises the surrounding cells and tissues [6]. Many studies have attempted to improve the clinical performance of PMMA bone cement by several methods [5,7–11]. Among them, incorporation of bioactive inorganic fillers such as bioactive glasses (BGs) [8,9] and glass–ceramics [10] or hydroxyapatite [11] into the PMMA matrix has been found to be an effective approach. Although these bioactive fillers can improve the bioactivity of PMMA cement, they are far from optimal, because large percentage of bioactive fillers may impair the mechanical strength and handling properties of PMMA [12], not to mention that apatite–wollastonite (A–W) glass–ceramic and hydroxyapatite lack sufficient biodegradability and osteostimulative activity [4].

BGs, such as the silicate glasses designated 45S5 and 13–93, have the ability to react with the body fluid and convert to hydroxyapatite, which leads to the formation of a strong bond with bone and soft tissue [13,14]. Recently, borate BGs, a novel class of BGs that substitutes partial silicate for borate, have been the focus for biomedical applications [14,15] due to their excellent bioactivity, biodegradation, osteoconductivity and osteoinduction [14,16]. It is easy to control the degradation rate of borate BGs by manipulating their composition to match up with the bone-regeneration rate, which is particularly useful for promoting the regeneration of bone [14]. Moreover, the compositional flexibility of borate BGs can be used to serve as a source of many of the minor elements such as strontium (Sr) that are known to favour bone growth [14,17].

Sr plays an important role in inhibiting bone resorption and stimulating bone formation [18,19]. Its mechanism relies on the ability of Sr^{2+} ions to stimulate the alkaline phosphatase (ALP) activity, the osteogenic-related gene expression of mesenchymal stem cells and the expression of osteoprotegerin [20]. In addition, Sr has been shown to enhance the proliferation and osteogenic differentiation of human osteoblast-like cells (MG-63) and bone marrow stromal cells as well as the expression of angiogenic factors, leading to a coupling between angiogenesis and osteogenesis [21]. Systemic administration of strontium ranelate was found to increase bone mineral density, reduce the incidence of hip and vertebral fractures in patients with osteoporosis [22] and improve the peri-implant bone volume and implant pull-out strength in animals [23]. However, the bioavailability of strontium ranelate is low (less than 20% by oral administration), and the use of strontium ranelate has been associated with adverse effects such as cutaneous hypersensitivity, venous thrombosis, chronic renal failure and osteomalacia [24]. Consequently, sustained local release of Sr^{2+} ions from implants may be more suited to systemic administration.

In this study, we aimed to attain better bone regeneration by doping Sr into borate BG and further incorporating it into PMMA to fabricate novel bioactive composite cements, namely Sr-doped borate bioactive glass (SrBG)/PMMA composite cements. In addition, we investigated the effect of SrBG on the self-setting behaviour and mechanical strength of the PMMA matrix to determine if it could comply with the requirements of International Organization for Standardization (ISO) 5833 [25] (implants for surgery—acrylic resin cements). Furthermore, we systematically evaluated (i) the ability of the SrBG/PMMA composite bone cement to induce apatite formation, (ii) the *in vitro* cellular response, namely adhesion, migration, proliferation and differentiation of MC3T3-E1 on the surface of SrBG/PMMA composite bone cement, and (iii) the bone-repair ability in a rat tibia model.

2. Material and methods

2.1. Preparation of poly(methylmethacrylate) cement and strontium-containing borate bioactive glass/poly(methylmethacrylate) composite cements

PMMA cement and SrBG/PMMA composite cements were prepared by mixing solid and liquid components at particular solid-to-liquid ratios. The solid component of SrBG/PMMA contained SrBG (10–50 µm) and PMMA (10–80 µm). SrBG (composition, $6Na_2O{\cdot}8\,K_2O{\cdot}8MgO{\cdot}16CaO{\cdot}6SrO{\cdot}27B_2O_3{\cdot}27SiO_2{\cdot}2P_2O_5$) was prepared by mixing the required amounts of Na_2CO_3, K_2CO_3, $MgCO_3$, $CaCO_3$, $SiCO_3$, SiO_2, H_3BO_3, NaH_2PO_4 (analytical grade; Sinopharm Chemical Reagent Co., Ltd, Shanghai, China), melting the mixture in a platinum crucible for approximately 1 h at 1200°C and quenching the melt between cold steel plates. The glass was crushed, ground in a steel mortar and pestle, and sieved in a stainless steel sieve to yield a particle size of 10–50 µm [26], and PMMA was purchased from Makevale Group (Ware, UK). The solid component was mixed using a three-dimensional motion mixer (GH-5 L; Ranged Machinery Co., Ltd, Jiangyin, China) to attain a homogeneous dispersion. The liquid component contained MMA (monomer, 3 ml) and DMPT (accelerator, 0.14 µl) (Sigma-Aldrich, St Louis, USA). Details of the PMMA cement and SrBG/PMMA composite cements are summarized in table 1.

2.2. Handling properties of poly(methylmethacrylate) cement and strontium-containing borate bioactive glass/poly(methylmethacrylate) composite cements

2.2.1. Self-setting properties

The setting properties of the PMMA cement and SrBG/PMMA composite cements were examined according to the ISO 5833 criteria [25]. The variation in temperatures during the setting reaction process was measured using a K-type thermocouple (Spectris, Shanghai, China) connected to data-acquisition equipment (STR90, Shuntong Instrument Co., Ltd, Huai'an city, China). Immediately after the cement paste was poured into a self-made Teflon mould under ambient conditions (23°C), the inner temperatures of the paste were measured and recorded at 5 s intervals for a total time of 25 min. The profile of temperature versus time was prepared to determine the peak temperature and setting time. The maximum temperature within the profile was assigned to the peak temperature during polymerization of the composite cement. The setting time was defined as the time point when the exothermic temperature increased to the mid-point between the ambient and peak temperatures and was determined using the following equation:

$$T_{set} = \frac{T_{max} + T_{amb}}{2}, \tag{2.1}$$

where T_{set} is the setting temperature, T_{max} the peak temperature and T_{amb} the ambient temperature. The measurements were repeated five times for reproducibility.

Table 1. Compositions of PMMA cement and SrBG/PMMA composite cements.

		solid parts (g)			
cements	filler loading (wt%)	PMMA powder (g)	SrBG (g)	liquid parts (ml)	S/L (S = PMMA + SrBG)
control (PMMA)	0	2	0	1	2 : 1
10SrBG/PMMA	10	2	0.2	1	2.2 : 1
20SrBG/PMMA	20	2	0.4	1	2.4 : 1
30SrBG/PMMA	30	2	0.6	1	2.6 : 1

2.2.2. Mechanical properties

To determine the mechanical strength of the prepared cements, cylindrical specimens with 12 mm height and 6 mm diameter were prepared for compression testing according to the ISO 5833 criteria. The compressive strengths of the PMMA cement and SrBG/PMMA composite cements were measured using a universal mechanical testing machine (AG-5KN; Shimadzu, Japan) at a cross-head speed of 20 mm min^{-1}. Rectangular specimens of dimensions 3.3 (thickness) × 75.0 (length) × 10.0 (width) mm were prepared for flexural testing according to the ISO 5833 criteria [25], along with a universal mechanical testing machine (AG-5KN; Shimadzu, Japan) at a constant cross-head speed of 5 mm min^{-1}. Six samples per group were tested to obtain an average value of the mechanical strength.

2.3. Bioactivity and ion release of poly(methylmethacrylate) cement and strontium-containing borate bioactive glass/poly(methylmethacrylate) composite cements

Cement specimens (10 mm diameter and 3 mm length) were set for 1 day and soaked in 30 ml of simulated body fluid (SBF) (calculated from the apparent surface area of the specimen according to a previous study [27]) in plastic containers at 37°C for 30 days. The specimens were washed with distilled water, dehydrated in a graded series of ethanol and dried at 60°C. The morphology of the mineralized layer on the surface of bone cements before and after soaking in SBF was observed using field emission scanning electron microscopy (FE-SEM; Nova NanoSEM 450, FEI, The Netherlands) at an acceleration voltage of 10 kV. The Ca/P ratio of the mineral layer was determined using energy dispersive X-ray spectrometry (EDS; Inca X-act, Oxford, UK).

The ion release profile of the SrBG/PMMA composite cements was evaluated by soaking the cements in phosphate-buffered saline (PBS) at 37°C. Cylindrical cement samples (10 mm diameter and 3 mm length) were set for 1 day and soaked in 30 ml PBS [27] in plastic containers. At each selected time point, 0.1 ml PBS was taken out carefully, cooled to room temperature and diluted 10-fold with deionized water. The ionic concentration of PBS was measured by inductively coupled plasma optical emission spectroscopy (Optima 7000DV, PerkinElmer, Waltham, MA, USA). The ionic concentration of three immersion samples was measured at each selected time, and the results were expressed as mean ± s.d.

2.4. *In vitro* evaluation of poly(methylmethacrylate) cement and strontium-containing borate bioactive glass/poly(methylmethacrylate) composite cements

2.4.1. Cell culture

The osteogenic MC3T3-E1 cell line used in these experiments was purchased from the cell bank of Chinese Academy of Sciences at Shenzhen, China. The cells were cultured in α-MEM (Corning, NY, USA) supplemented with 10% fetal bovine serum (FBS; Corning, NY, USA) plus 100 U ml^{-1} penicillin and 100 μg ml^{-1} streptomycin sulfate. When approximately 80% confluence was reached, the cells were trypsinized in 0.25% pancreatic enzymes. Cells of generations 11, which were cultured at 37°C in a humidified atmosphere of 5% CO_2, were used for all the cell culture experiments.

2.4.2. Cytotoxicity

An MTT assay was performed to determine the cytotoxicity of the PMMA cement and SrBG/PMMA composite cements through co-culture of MC3T3-E1 cells with extracts of the PMMA cement and SrBG/PMMA composite cements. The extracts were prepared according to the ISO 10993 specifications [28] (biological evaluation of medical devices). The cylindrical cements (10 mm (diameter) × 3 mm (thickness)) were first treated with 75% ethanol and then with PBS for 24 h. Subsequently, the cement samples were soaked in α-MEM (ratio of cement sample to medium, 1/5 (w/v)) at 37°C for 24 h. The medium was then used as the extract (marked as 'extract') in the following cell culture without further filtration. The MC3T3-E1 cells were seeded into a 96-well plate containing 200 μl per well of growth medium at a density of 1.0×10^3 cells per well and incubated for 24 h to allow cell attachment. Thereafter, the medium was replaced with 200 μl of the extracts of PMMA cement and SrBG/PMMA composite cements. After 24 h of culture, 20 μl MTT solution (5 mg ml^{-1}) (GBCBIO Technology Inc., Guangzhou, China) was added to each well and incubated at 37°C for 4 h to form formazen, which was then dissolved using dimethyl sulfoxide. The optical density of each well was measured at 570 nm with a plate reader (BioTek Synergy4, Winooski, VT, USA). The α-MEM without extract was used as the control.

2.4.3. Cell adhesion

The MC3T3-E1 cells were seeded on the surface of the cements with 10 mm diameter and 3 mm thickness at a density of 5.0×10^4 cells per well. After 3 days of incubation, the surfaces of the cement samples were rinsed with PBS to remove the non-adherent cells. The remaining cells were fixed using 2.5% glutaraldehyde in cacodylate buffer (Guangzhou Chemical Reagent Factory, Guangzhou, China) and washed with cacodylate buffer containing sucrose. After dehydration with gradient alcohol and sputter-coating with gold, the morphology of the cells was observed using FE-SEM at an acceleration voltage of 10 kV.

2.4.4. Cell migration

A scratch assay was used to detect the effects of the cements on horizontal migration. A total of 5×10^4 cells were added to each well of 6-well plates and grown into a confluent monolayer. A 'scratch' was introduced by scraping the monolayer with a P200 pipette tip (Gilson, Inc., Middleton, WI, USA). The debris was removed, and the edge of the scratch was smoothened

by washing twice with D-Hank's solution (Beijing Solarbio Science & Technology Co., Ltd, Beijing, China). Extracts of the cements were prepared as described in §2.4.2. The extracts were supplemented with 0.5% FBS and poured into a plate; basal medium with 0.5% FBS served as the control. Each group had 10 duplicates. After incubation at 37°C for 8–18 h, the plate was observed at the selected time points using an inverted phase-contrast microscope (CKX41, Olympus (China) Co., Ltd, Shanghai, China).

A transwell assay was performed to detect the effects of the cements on vertical migration. A total of 1×10^5 cells in a medium starved of serum were added to the top chamber of cell culture inserts (8 mm pore size) in a 24-well plate, and three extracts supplemented with 0.5% FBS were added to the bottom chambers; basal medium with 0.5% FBS served as the control. Each group had 10 duplicates. After incubation for 12 h at 37°C, the inserts were removed, and the remaining migrated cells were agitated gently with a pipette. After fixation in methanol for 30 s, the migrated cells were stained with crystal violet (Beyotime, Shanghai, China) and counted. Ten observation fields were calculated for each duplicate.

2.4.5. Alkaline phosphatase activity

The MC3T3-E1 cells were seeded on the surface of the cements with 10 mm diameter and 3 mm thickness at a density of 2.0×10^5 cells per well in a six-well plate. After culturing for 3 days at 37°C, the medium was replaced with a self-made osteogenic differentiation medium, which contains dexamethasone, β-glycerophosphate disodium salt hydrate, L-ascorbic acid 2-phosphate sesquimagnesium salt hydrate (Sigma-Aldrich), to induce differentiation of MC3T3-E1 cells. At 7 and 14 days of incubation, the medium was removed and the cell monolayer was washed twice with PBS. The cells were then treated with cold Triton X-100 (Sigma-Aldrich) for 1 h under agitation to extract the ALP. Aliquots of the mixture were taken for estimation of the protein concentration. The ALP assay was performed according to the manufacturer's protocol using an ALP assay kit (Beyotime, Shanghai, China). Six duplicates were measured at each time point.

2.4.6. Collagen secretion

Collagen secretion of the MC3T3-E1 cells on the surface of cements was quantified using the Sirius Red staining method [29]. The MC3T3-E1 cells were seeded on the samples (four replicates) onto 24-well plates at a density of 1×10^4 cells per well. At 7 and 14 days of incubation, the samples were washed thrice with PBS and fixed in 4% paraformaldehyde. Following three rinses in PBS, the samples were stained for collagen secretion using a 0.1% solution of Sirius Red (Sigma-Aldrich) in saturated picric acid for 18 h. After washing with 0.1 M acetic acid until no red colour appeared, the stain on the samples was eluted in 500 ml of the solution (0.2 M NaOH/methanol, 1 : 1). The optical density was measured at 540 nm with an enzyme-labelling instrument (BioTek Synergy4).

2.5. *In vivo* evaluation of poly(methylmethacrylate) cement and strontium-containing borate bioactive glass/poly(methylmethacrylate) composite cements

2.5.1. Animal experiments and implantation procedure

The study protocol was approved by the Animal Care Committee of Shenzhen Institute of Advanced Technology, Chinese Academy of Sciences. All experiments were conducted in accordance with the guidelines of the local Animal Welfare Committee.

Sixteen male Sprague–Dawley rats (three months old, average weight 350 g) underwent surgery under general inhalation anaesthesia using a Univentor 400 anaesthesia unit (Univentor Ltd, Zejtun, Malta) and isoflurane (Isoba® Vet; Schering-Plough Ltd, Uxbridge, UK) inhalation (2.3%, with airflow of 450 ml min^{-1}). All animals received a local injection of xylocaine (Shanghai Pharmaceutical Industries Co., Ltd, Shanghai, China) at the site of implantation and a subcutaneous injection of an analgesic (Temgesic; RB Pharmaceuticals, Berkshire, UK; 0.024 mg kg^{-1} body weight) post-operatively and twice a day for 2 days in order to minimize the operative and post-operative pain. Each leg was shaved and cleaned with 5 mg ml^{-1} chlorohexidine in 70% ethanol, and the medial aspect of the medial tibial metaphysis was exposed. The implantation sites were prepared using 2.5 mm diameter round burs under profuse irrigation with saline.

The pre-setting sample of SrBG/PMMA composite cement (denoted as 30SrBG/PMMA as summarized in table 1) and commercial PMMA cement (OSTEOPAL® V, Heraeus, Germany) were implanted into the medial metaphysis of the tibia in both hind legs of the rats. All animals were allowed free post-operative movement with food and water ad libitum. The retrieval procedures were performed after eight and 12 weeks of implantation. At each retrieval time point, the animals were sacrificed using an overdose of barbiturate (Mebumal; ACO Läemedel AB, Solna, Sweden), and the implants in the tibial metaphysis were exposed. Thereafter, the implants were retrieved and preserved according to the analytical procedures as described in §§2.5.2. and 2.5.3.

2.5.2. Histological examination

Sections (approx. 5 μm thick) in the longitudinal direction of the rat tibia were stained with Giemsa stain and examined using transmitted light microscopy. The excised tibial specimens of the animals sacrificed at eight and 12 weeks post-implantation were fixed in 10% formaldehyde and dehydrated in a graded series of ethanol. In the subsequent days, the excised tibial specimens were embedded in PMMA using alcohol–PMMA mixtures with increasing concentrations of the embedding media Technovit 7200 VLC (Heraeus Kulzer GmbH, Wehrheim, Germany). After hardening, 20 mm sections were cut from the middle of the cement plug on the tibia and ground to a thickness of 70 mm using a grinding machine (EXAKT400 CP Micro Grinding System, Norderstedt, Germany). The surface was then polished with #4000 garnet papers (Sinopharm Chemical Reagent Co., Ltd). At the end, the sections were stained with Giemsa stain for histological observation under a light microscope (Axioskop 40; Carl Zeiss, Jena, Germany) connected to a digital camera (AxioCam MRc5 Carl Zeiss).

2.5.3. Micro-computed tomography

The rat tibiae of the animals sacrificed at eight and 12 weeks post-implantation were fixed in 4% paraformaldehyde, and the morphology of the reconstructed tibia was assessed using micro-computed tomography (micro-CT; Skyscan 1176, Kontich, Belgium). Scanning was performed at a resolution of 18 μm. The micro-CT images were reconstructed using the Feldkamp convolution back-projection algorithm and segmented into binary images using adaptive local thresholding.

2.6. Statistical analysis

Data are presented as mean ± s.d. Statistical analysis was performed using one-way analysis of variance followed by Tukey's *post hoc* test, with the level of significance set at $p < 0.05$.

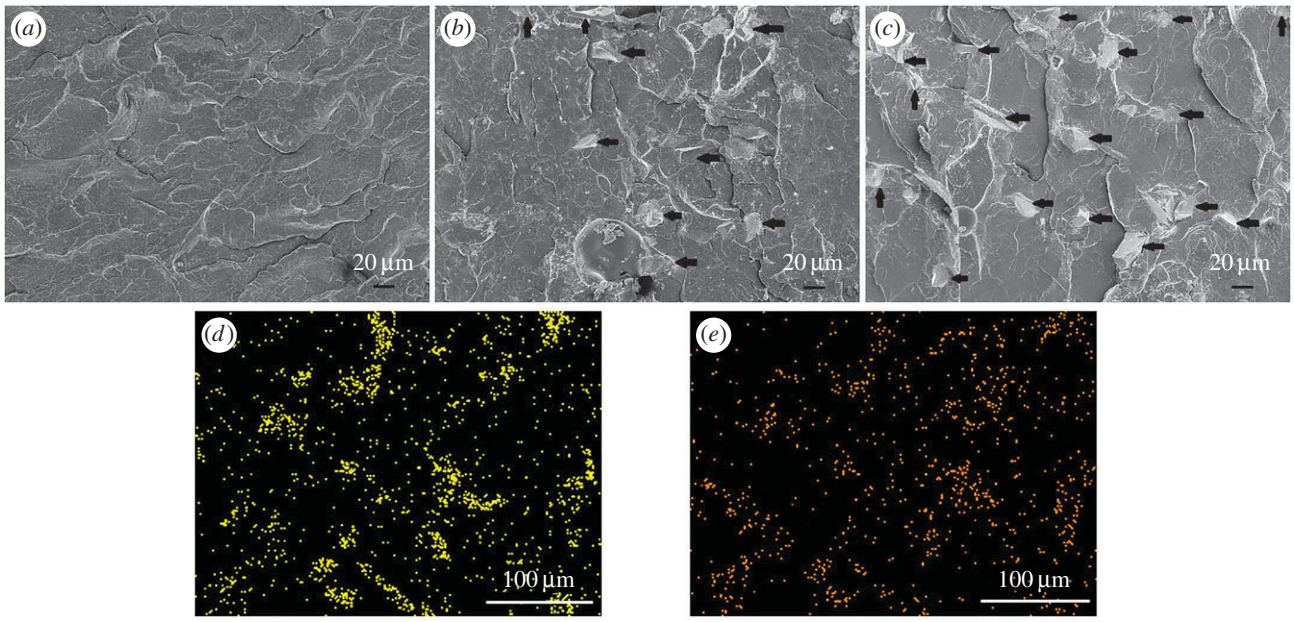

Figure 1. The cross-sectional microstructure of (*a*) PMMA bone cement, (*b*) 10SrBG/PMMA and (*c*) 30SrBG/PMMA composite cements (the black arrows indicate the SrBG particles). EDS analysis of the elements (*d*) Si and (*e*) Ca shows that SrBG particles are dispersed in the 30SrBG/PMMA composite cement. (Online version in colour.)

3. Results

3.1. Characterization of strontium-containing borate bioactive glass/poly(methylmethacrylate) composite cements

Figure 1 shows the cross-sectional microstructure of the PMMA cement and 10SrBG/PMMA and 30SrBG/PMMA composite cements. The SrBG powders interacted solidly within the PMMA matrix (figure 1*b*,*c*), and there were some pores within the SrBG/PMMA composite cements. The EDS analysis (figure 1*d*,*e*) revealed that silicon and calcium existed within the PMMA matrix. Synergistically, the microstructure and EDS analysis of the SrBG/PMMA composite cements demonstrated the distribution of SrBG particles within the PMMA matrix.

3.2. Handling properties of strontium-containing borate bioactive glass/poly(methylmethacrylate) composite bone cements

3.2.1. Self-setting properties

The peak temperature of polymerization of 10SrBG/PMMA, 20SrBG/PMMA and 30SrBG/PMMA (figure 2*a*) decreased with the amount of SrBG in cements (84.4 $\pm$ 1.85°C, 73.2 $\pm$ 2.14°C and 65.5 $\pm$ 2.85°C, respectively), and the peak temperature of the SrBG/PMMA composite cements was evidently lower than that of PMMA cement (88.7 $\pm$ 2.23°C) and maximum temperature value specified by the ISO 5833 (90°C) [25]. The setting times for the cements increased with the SrBG content, from 6.67 $\pm$ 0.26 min for PMMA cement to 10.89 $\pm$ 0.36 min for 30SrBG/PMMA composite cement (figure 3*b*), but were still within the appropriate setting times for operation in a surgical room (6–15 min).

3.2.2. Mechanical properties

The results of the mechanical test are depicted in figure 3. The compressive strength of the specimens was 83.59 $\pm$ 5.65, 89.62 $\pm$ 6.99, 78.31 $\pm$ 4.55 and 80.72 $\pm$ 3.03 MPa for PMMA, 10SrBG/PMMA, 20SrBG/PMMA and 30SrBG/PMMA cements, respectively (figure 3*a*), all of which were higher than the minimum value of compressive strength required by the ISO 5833 [25] criterion (greater than 70 MPa). The flexural strength of cements decreased with the increase in SrBG content, which was 61.03 $\pm$ 3.44, 55.62 $\pm$ 2.21, 53.13 $\pm$ 2.68 and 50.1 $\pm$ 1.69 MPa for PMMA, 10SrBG/PMMA, 20SrBG/PMMA and 30SrBG/PMMA cements, respectively (figure 3*b*). The flexural strength of all SrBG/PMMA composite cements satisfied the ISO 5833 [25] criterion (greater than 50 MPa), although the flexural strength of the 30SrBG/PMMA composite cement was only slightly higher than the minimum value. However, the flexural modulus of the SrBG/PMMA composite cement (figure 3*c*) increased with the SrBG content in the cement, and all values of the flexural modulus were far beyond the critical value of 1800 MPa set by the ISO 5833 [25] criterion.

3.3. Bioactivity and ion release of strontium-containing borate bioactive glass/poly(methylmethacrylate) composite cements

When immersed in an aqueous phosphate solution, SrBG degraded and converted to hydroxyapatite and released boron (B) and the glass network modifiers (such as Ca^{2+} and Sr^{2+}) into the solution [30]. The Ca^{2+} released from the glass then reacted with the phosphate ions to form an amorphous calcium phosphate or hydroxyapatite-like material, which imparted bioactivity to the cements.

Figure 4 shows the X-ray diffraction patterns of the SrBG/PMMA composite cements after soaking in SBF for 30 days. The diffraction peaks for low crystallinity of the hydroxyapatite phase (Standard Card No. JCPD 24-0033) were detected at 2θ 26° and 32° for the SrBG/PMMA composite cements after soaking in SBF. Figure 5 shows the results of SEM and EDS analysis for the surface of the cements after soaking in SBF for 30 days. No or very little particle deposition was

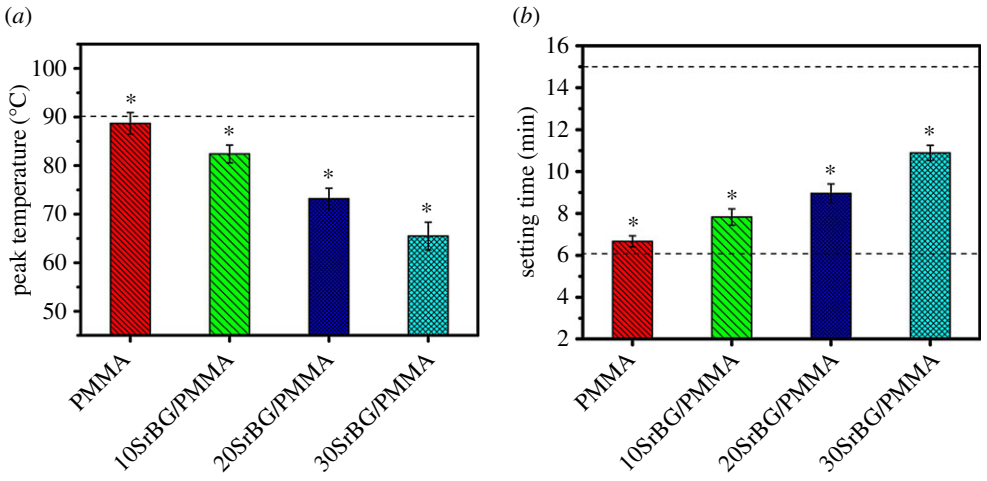

Figure 2. (*a*) Peak temperature of the cement paste during the setting process and (*b*) setting time of the cements (dotted line indicates the International Organization for Standardization 5833 value). The results are presented as mean ± s.d., $n = 5$, *t*-test; $^*p < 0.05$. (Online version in colour.)

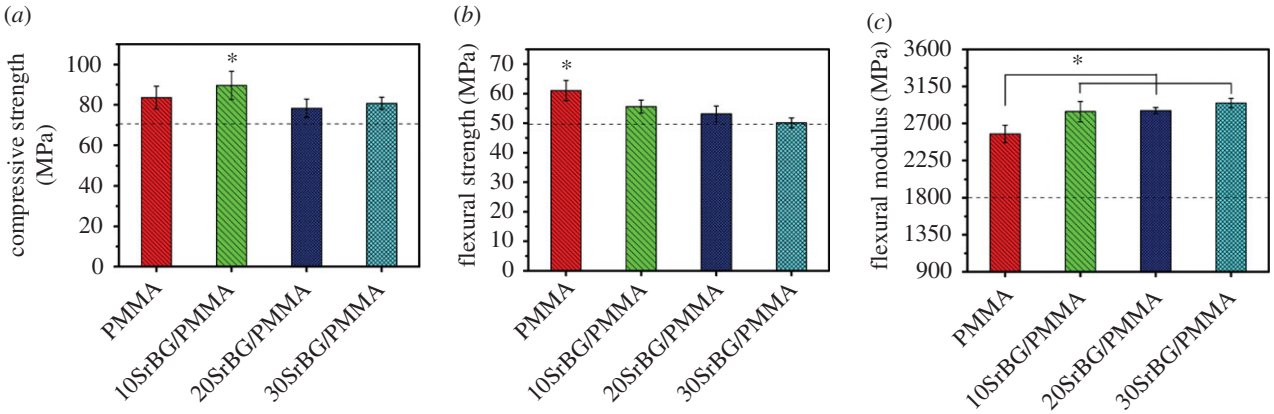

Figure 3. (*a*) Compressive strength, (*b*) flexural strength and (*c*) flexural modulus of the cements (dotted line indicates the International Organization for Standardization 5833 value). The results are presented as mean ± s.d., $n = 5$, *t*-test; $^*p < 0.05$. (Online version in colour.)

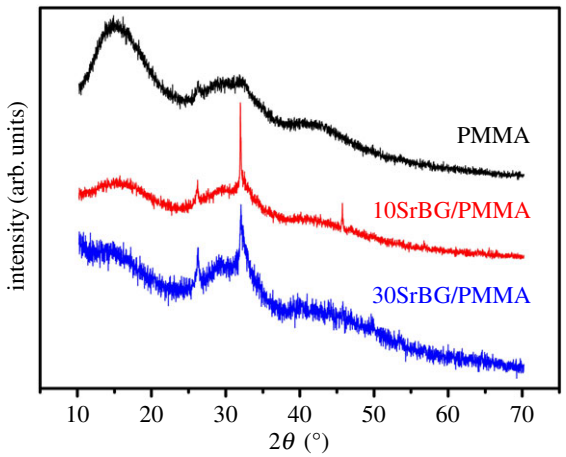

Figure 4. X-ray diffraction patterns of pure PMMA, 10SrBG/PMMA and 30SrBG/PMMA cements after immersion in simulated body fluid for 30 days. (Online version in colour.)

observed on the surface of the PMMA cement (figure 5*a*). EDS analysis demonstrated that there were no Ca and P elements (figure 5*g*). By contrast, newly formed clusters of particles were observed on the surface of the SrBG/PMMA composite cements after exposure to SBF (figure 5*b*,*c*). Coverage of the deposition layer on the surface increased with an increase in the SrBG content. Only a small number of granular crystals appeared on the surface of the 10SrBG/PMMA composite cement. As the SrBG content increased up to 30%, the newly formed apatite layer had covered more surface of the sample (figure 5*c*). Higher magnification images showed that the newly formed apatite layers on the composite cements were composed of aggregates of nanocrystals with worm-like morphology (figure 5*e*,*f*). EDS analysis confirmed that the Ca/P ratio of the formed apatite on the surface of the 30SrBG/PMMA bone cement was 1.298 (figure 5*h*).

The changes in the concentrations of B and Sr ions of PBS solutions during the immersion test are shown in figure 6. The release profile of B and Sr in 10SrBG/PMMA and 30SrBG/PMMA cements showed a similar tendency, i.e. a low release rate during the initial 14 days, which increased tremendously to a much higher rate at the later stages of immersion time.

3.4. Response of MC3T3-E1 cells *in vitro*

3.4.1. Cell adhesion and cell proliferation

After 3 days of culture, all the cements supported MC3T3-E1 cell attachment (figure 7). On the surfaces of the SrBG/PMMA composite cements, the cells displayed discernible filopodia (figure 7*a*,*b*,*d*,*e*). MTT analysis

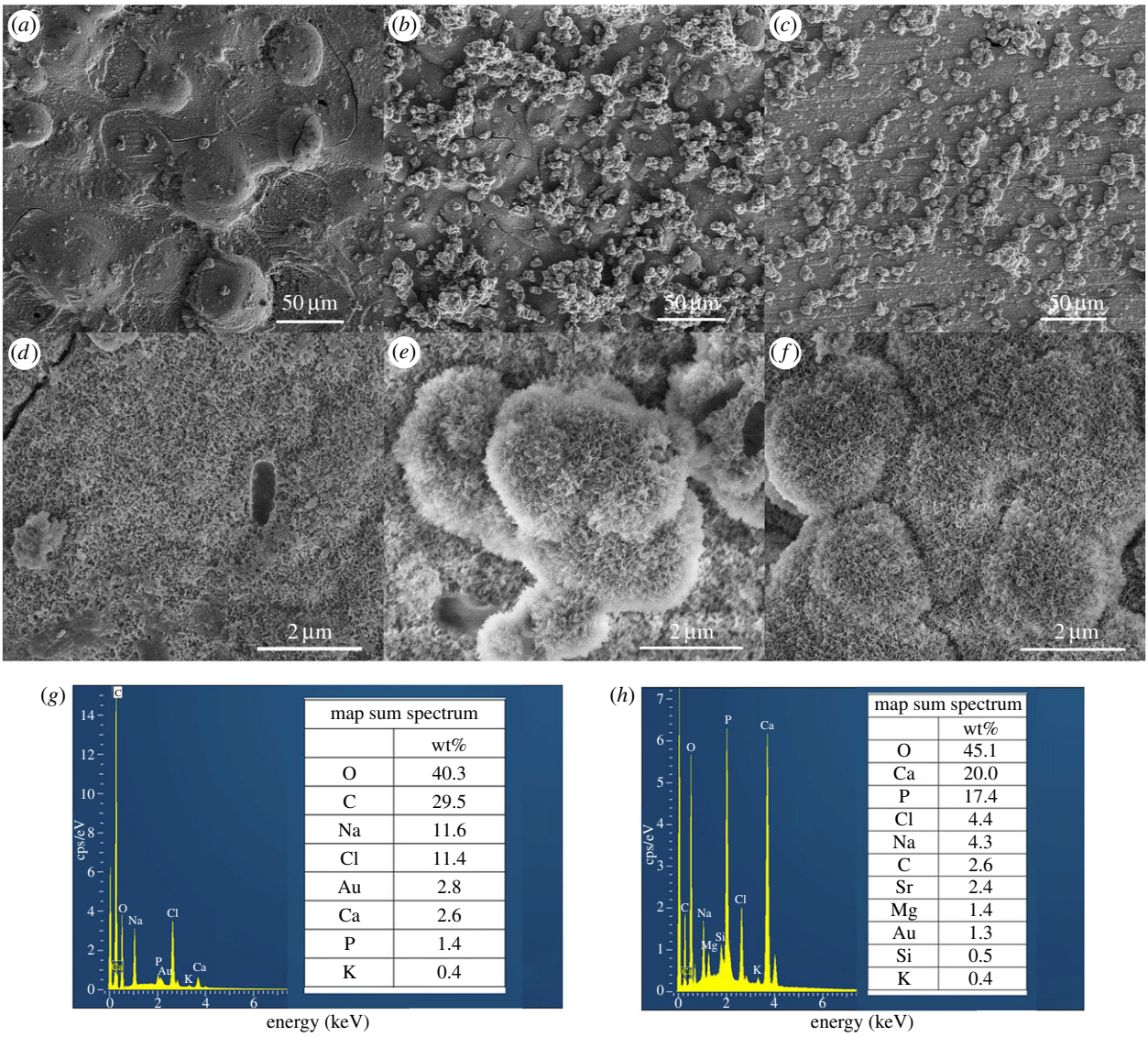

Figure 5. Scanning electron microscopy images and EDS analysis of PMMA cement and SrBG/PMMA composite cements after immersion in simulated body fluid for 30 days. (*a*,*d*) PMMA, (*b*,*e*) 10SrBG/PMMA, (*c*,*f*) 30SrBG/PMMA, (*g*) EDS analysis of PMMA, (*h*) EDS analysis of 30SrBG/PMMA. (Online version in colour.)

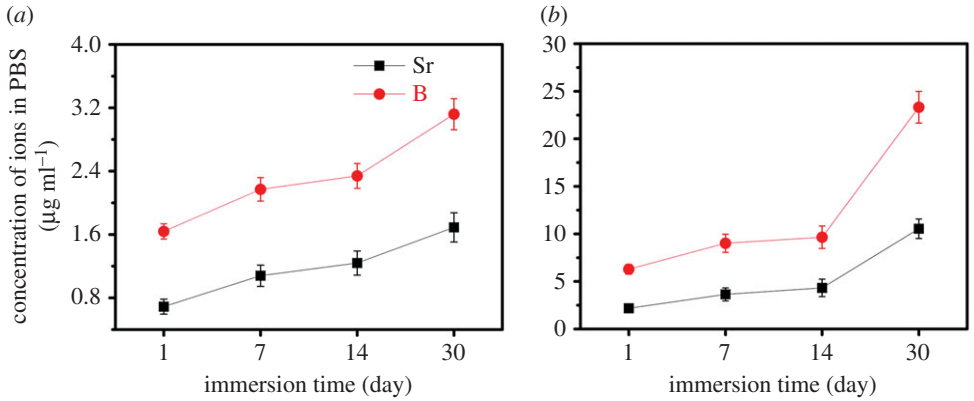

Figure 6. Cumulative amount of strontium and boron released from (*a*) 10 SrBG/PMMA composite and (*b*) 30SrBG/PMMA composite cements as a function of immersion time in PBS. The results are presented as mean ± s.d. (Online version in colour.)

(figure 8) showed that the extract of the SrBG/PMMA composite cements had a much higher relative growth rate (RGR) than that of the PMMA cement after culture for 3 and 7 days. Overall, the RGR of the extract of all cements was above the dashed line in figure 8, yielding acceptable RGRs according to ISO 10993 [28]. Of note, with the increase in SrBG in the composite cements, the RGR first increased and then declined. This may be due to the cytotoxicity of the higher alkalinity of the microenvironment caused by ion release from SrBG during the conversion and degradation process of the 30SrBG/PMMA composite cement [30].

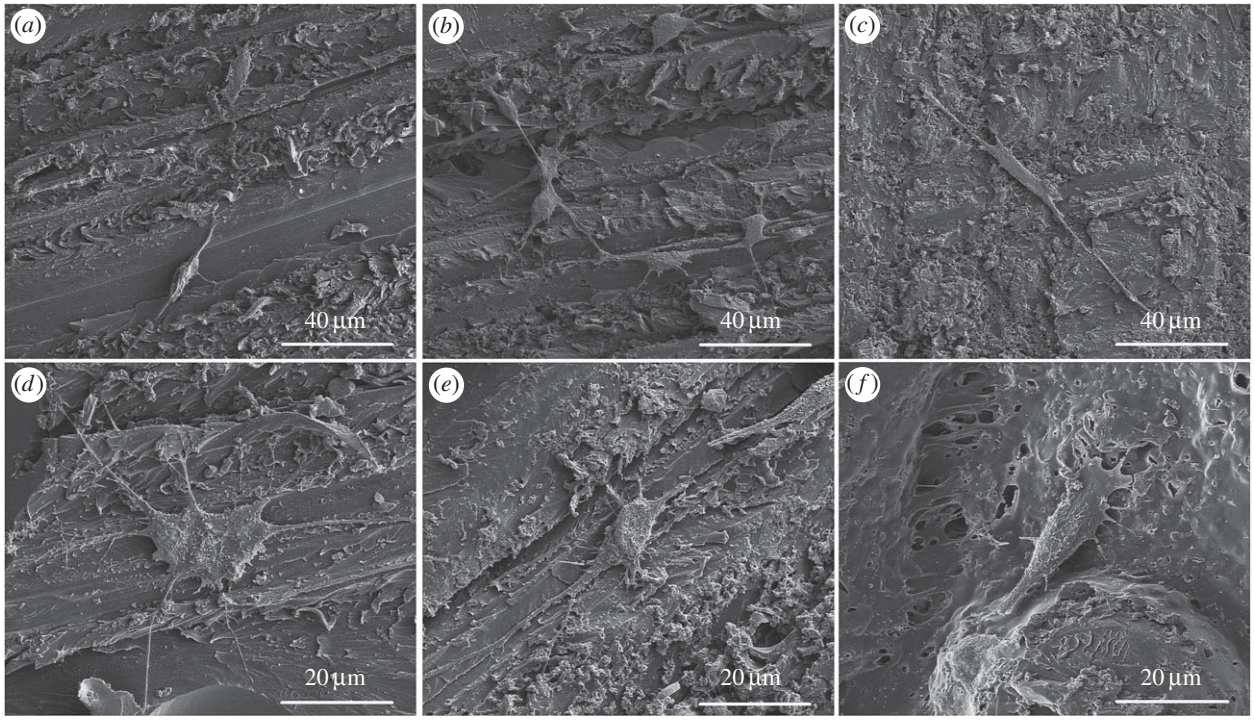

Figure 7. Morphology of MC3T3-E1 cells incubated for 3 days on the surface of PMMA and the SrBG/PMMA composite cements. (*a,d*) 30SrBG/PMMA, (*b,e*) 10SrBG/PMMA, (*c,f*) PMMA.

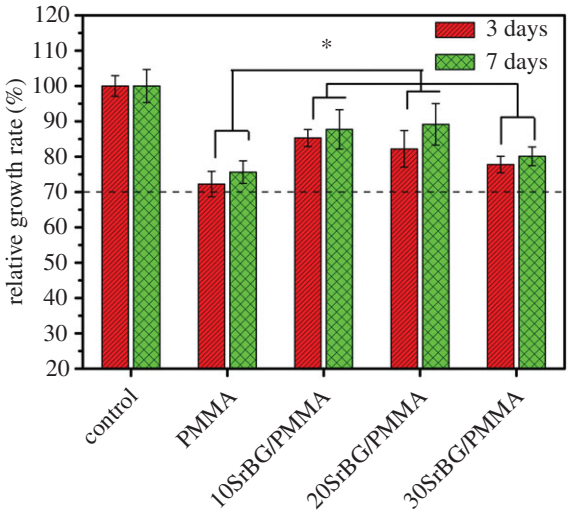

Figure 8. RGR of MC3T3-E1 cells after culture with the PMMA cement and SrBG/PMMA cements (dashed line indicates the acceptable RGR). *Significant difference between groups ($p < 0.05$). (Online version in colour.)

3.4.2. Cell migration

According to the results of the cell-migration assay (figure 9), the PMMA cement showed a significant decrease in horizontal migration ($p < 0.05$, $n = 10$). Moderate inhibition was detected for the 30SrBG/PMMA composite cement, whereas slight promotion was noted for the 20SrBG/PMMA composite cement. There was no significant difference between the 10SrBG/PMMA and 20SrBG/PMMA composite cements ($p < 0.05$, $n = 10$; figure 9*a*). All the cements had enhanced vertical migration of MC3T3-E1 cells, but the 20SrBG/PMMA composite cement showed highest promotion on vertical migration of MC3T3-E1 cells (figure 9*b*).

3.4.3. Alkaline phosphatase activity

The ALP activities of MC3T3-E1 cells after culture on the cements for 7 and 14 days are shown in figure 10*a*. The SrBG/PMMA composite cements had higher ALP activities than the PMMA bone cement ($p < 0.05$) at both 7 and 14 days. Further, among all composite cements, the 10SrBG/PMMA cement had the highest ALP activity. There were no significant differences in the ALP activity among the different culture times for all the SrBG/PMMA composite cements ($p > 0.05$).

3.4.4. Collagen secretion

Significant enhancements in collagen secretion (figure 10*b*) were observed in each SrBG/PMMA composite cement ($p < 0.05$, $n = 10$). However, the 10SrBG/PMMA and 20SrBG/PMMA composite cements showed a higher promotion than the 30SrBG/PMMA composite cement, but there was no significant difference between them ($p > 0.05$).

3.5. *In vivo* osteointegration of strontium-containing borate bioactive glass/poly(methylmethacrylate) composite cements

3.5.1. Histological evaluation

Giemsa surface staining sections of the overview of the rat tibia (figure 11*a–d*) show that after implantation for eight and 12 weeks, the 30SrBG/PMMA composite cements were well tolerated in the defect sites, and there were no signs of rejection, necrosis or infection. No bone resorption was noted around the 30SrBG/PMMA composite cement implant. The surface of the 30SrBG/PMMA composite cement was in intimate contact with the bone for most of the surface without any intervening soft tissue between the 30SrBG/PMMA composite cement and the host bone. Furthermore, more newly formed trabecular bone was visible around the 30SrBG/PMMA composite cement with a longer implantation time. Notably, the commercial PMMA

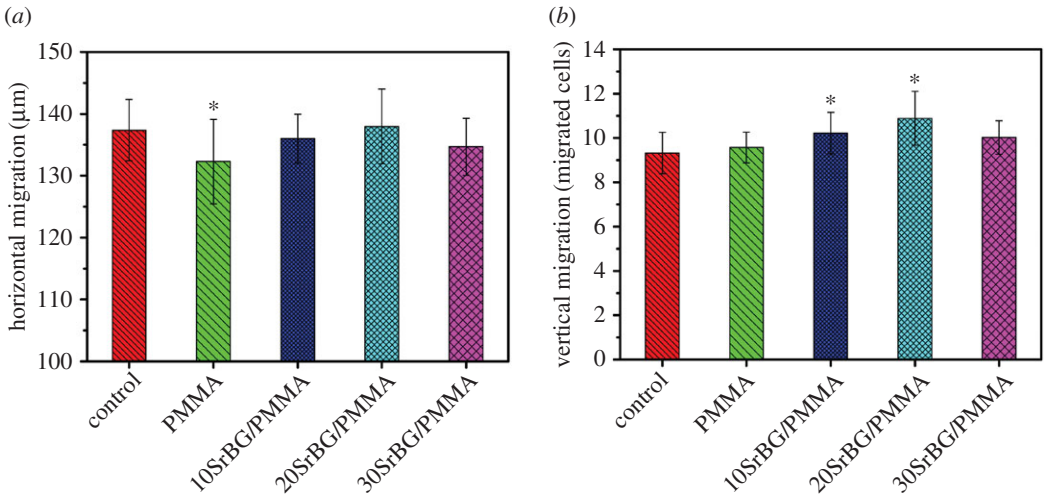

Figure 9. (*a*) Horizontal migration and (*b*) vertical migration of MC3T3-E1 cells after culture with the PMMA cement and SrBG/PMMA composite cements. *Significant difference between groups ($p < 0.05$). (Online version in colour.)

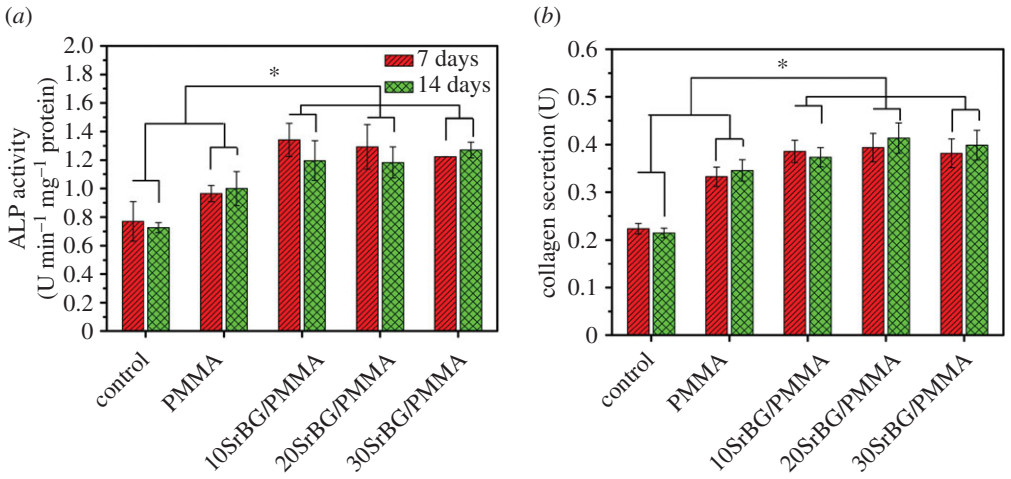

Figure 10. (*a*) ALP activities and (*b*) protein secretion of MC3T3-E1 cells after culture with the PMMA cement and SrBG/PMMA composite cements. *Significant difference between groups ($p < 0.05$). (Online version in colour.)

cement evoked an inflammatory response and foreign body reaction in the surrounding bony tissues.

Details of the bone–cement interface were further assessed using histomorphometric analysis after implantation (figure 11*e–h*). New-bone formation was visible on the superficial surface of the 30SrBG/PMMA composite cement. An intervening soft tissue layer of approximately 10–100 μm thickness was observed at the bone–PMMA cement interface. There were more areas of intimate contact between the surface of the SrBG/PMMA composite cement and the bone compared with that seen with PMMA cement (figure 11*e–h*).

3.5.2. Micro-computed tomography measurement

Figure 12 shows the three-dimensional reconstructed images and sagittal section images of rat tibia with implantation of PMMA cement and 30SrBG/PMMA composite cement for eight and 12 weeks. Interestingly, a layer of circular new bone formed around the implant at the interface between the 30SrBG/PMMA composite cement and the host bone at eight and 12 weeks post-implantation, whereas the PMMA cement showed no sign of new-bone formation. To our knowledge, circular new-bone formation at the implant–bone interface is rare with bioactive fillers/PMMA composite cements [2,5–9]. This finding demonstrated that the borate BG had excellent osteoinduction. The per cent bone volume of PMMA cement and the 30SrBG/PMMA composite cement at different implantation times is shown in figure 12*c*. The per cent bone volume of the 30SrBG/PMMA composite cement ($21.06 \pm 6.34\%$ and $33.94 \pm 4.84\%$ at eight and 12 weeks post-implantation, respectively) and the PMMA cement ($8.75 \pm 4.09\%$ and $12.46 \pm 3.87\%$ at eight and 12 weeks post-implantation, respectively) increased with implantation time. Together, these results suggested that the 30SrBG/PMMA composite cement had a high ability of osteoinduction and could induce bone formation around the implants.

4. Discussion

In this study, SrBG was incorporated as the reinforcement phase and bioactive filler of a PMMA cement to enhance osteointegration and osteostimulation of PMMA for expanding its application in orthopaedics. The SrBG/PMMA composite cements were bioactive, and their setting time and mechanical strength complied with the ISO 5833 criteria. Moreover, the peak temperature during setting of the

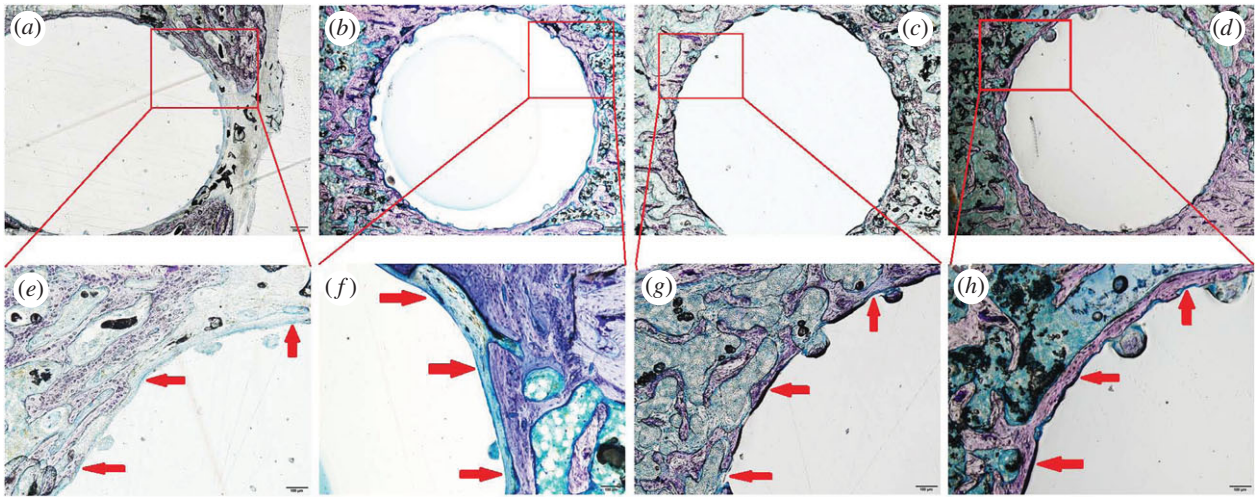

Figure 11. Giemsa surface staining of the overview (40×) and the bone–cement interface (200×) of rat tibia after implantation of PMMA cement and SrBG/PMMA composite cement. Fibrous tissue is stained blue with Giemsa stain. (*a*,*b*) Rat tibia with implantation of PMMA cement at eight and 12 weeks (around the PMMA cement, a layer of soft tissue is seen in most parts of the bone–cement interface); (*c*,*d*) rat tibia with implantation of SrBG/PMMA composite cement at eight and 12 weeks (in many areas around the SrBG/PMMA composite cement, i.e. 30SrBG/PMMA cement, a good bonding to the bone is seen); (*e*,*f*) implant–bone interface with implantation of PMMA cement at eight and 12 weeks; (*g*,*h*) implant–bone interface with implantation of SrBG/PMMA composite cement at eight and 12 weeks. Red arrows indicated the implant–bone interface. (Online version in colour.)

composite cements was lower than that observed in the polymerization of pure PMMA cement. Furthermore, the SrBG/PMMA composite cements could promote adhesion, migration, proliferation, differentiation and collagen secretion from pre-osteoblastic MC3T3-E1 cells *in vitro* and induce new-bone formation in a rat tibia model *in vivo*.

4.1. *In vitro* properties of strontium-containing borate bioactive glass/poly(methylmethacrylate) composite cements

The self-setting properties are key characteristics in the application of bone cements [31]. The SrBG/PMMA composite cement showed a lower peak temperature than PMMA cement (88.7°C) and the ISO 5833 standard [25] (90°C), which improves the biocompatibility of the cement [4]. In addition, the 30SrBG/PMMA composite cement showed the most suitable setting time (10.89 ± 0.36 min) among the cements [25], confirming the superior self-setting properties of the 30SrBG/PMMA composite cement [31,32].

With regard to the repair of large bone defects that can present in load-bearing bones, although the target mechanical properties of the implants are not well established, a commonly used guideline is that the strength of the implant should match that of the host bone [33]. The compressive strength and flexural strength of all the SrBG/PMMA composite cements after setting were higher than the minimum value required by ISO 5833 [25] (70 MPa) and much higher than the compressive strength of calcium phosphate cement [33]. In comparison, the compressive strengths of human trabecular bone and cortical bone are 2–12 MPa and 100–150 MPa, respectively [34], confirming that the SrBG/PMMA composite cement is a promising implant for repairing loaded bone at some defect sites [35]. When immersed in SBF, the SrBG/PMMA composite cements showed the formation of hydroxyapatite on the surface of the cement and the dissolution of ions such as B and Sr into PBS, which confirmed the bioactivity. Results of X-ray diffraction and SEM showed that the converted hydroxyapatite product was not fully crystallized or that the crystallite size was in the nanoscale range. Because of their higher surface area and degradation rate, these partially crystallized or nanoscale hydroxyapatite particles may be beneficial for cell crawling and migration [17].

Attachment and spreading of cells belong to the first phase of the cell/material interaction. The material characteristics can influence cellular response when cells contact the surface of biomaterials [4,36]. In this study, both PMMA and SrBG/PMMA composite cements were able to support cell adhesion and proliferation; however, the cells on the surface of the SrBG/PMMA composite cements showed better cell growth, suggesting no cytotoxicity of ions released from the SrBG/PMMA composite cements. When compared with MC3T3 cells cultured with PMMA, those cultured with SrBG/PMMA composite cements showed a significantly higher increase in cell vertical migration, ALP activity and collagen secretion. The improvement of cell proliferation, bone-related differentiation, collagen secretion and cell vertical migration may be related to the formation of an apatite layer [4,37], which favours the cell proliferation and differentiation. The ionic products (such as BO_3^{3-}, Sr^{2+}, Ca^{2+} and Si^{4+}) released from SrBG within the composite cements could be also beneficial for osteoblast attachment, proliferation and differentiation, as borate BG has a stimulatory effect on bone-related cells [14].

4.2. Repair of bone defects *in vivo*

For a bioactive cement to replace PMMA bone cement, it should have similar handling properties; better mechanical characteristics; and most importantly, high osteoconductivity and osteoinduction [4]. Bone cement with bioactivity can bond directly and solidly to living bone and strengthen the bone–cement interface, which is considered weak in bone–cement–implant constructs [38]. According to the results of the histological staining, there was no noticeable intervening soft tissue layer between the composite cements and the host

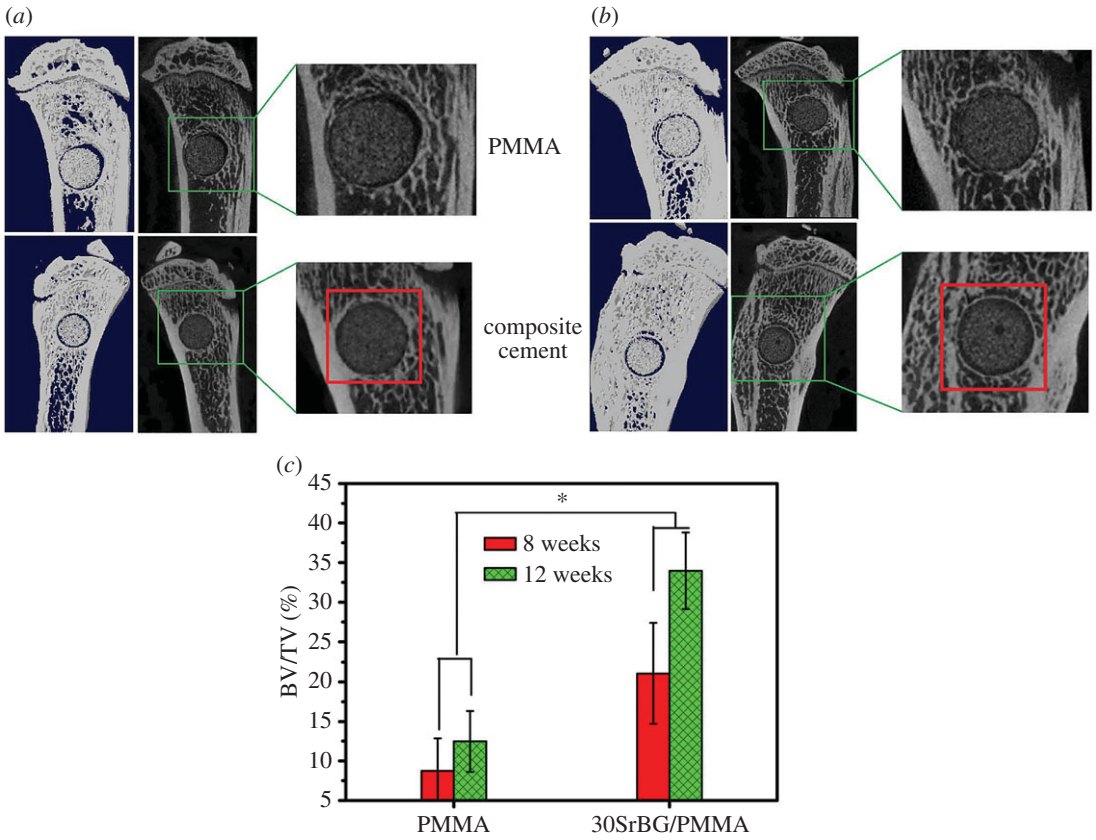

Figure 12. Micro-CT evaluation of bone regeneration in the rat tibia defects with implantation of PMMA cement and 30 SrBG/PMMA composite cement for (*a*) eight and (*b*) 12 weeks. Three-dimensional reconstructed images and sagittal images by micro-CT imaging of the area surrounding the cement implants, showing newly formed bone around the interface between the cement implant and host bone for (*a*) eight and (*b*) 12 weeks (area outlined in red); (*c*) bone volume/total volume (BV/TV) in the defects implanted with 30SrBG/PMMA composite cement with different post-implantation times. Values are presented as mean $\pm$ s.d.; $n = 3$. *Significant difference between groups ($p < 0.05$). (Online version in colour.)

bone, which was beneficial for formation of a tight bond between the host bone and the composite cements. The SrBG in composite cements had significantly enhanced osteogenic capability at the interfacial areas, stimulated greater bone formation around the interface of the composite cement implants and showed excellent osteoinduction. The improved osseointegration may improve fixation of implants and reduce bone resorption, thereby inducing the formation of new bone, which can provide a stable interface to avoid implant failure [23,39]. Our *in vivo* results are in agreement with those of previous studies and showed better bone formation than new PMMA-based bioactive bone cements with amphiphilic phosphorylated 2-hydroxyethylmethacrylate [40] and bioactive PMMA-based cements with silicate bioceramic [4] and A–W glass ceramic [41].

Our results suggest that incorporation of SrBG into the PMMA matrix could provide a more beneficial microenvironment for cell attachment, proliferation and differentiation and lead to a higher osteogenic capability in a rat tibia model *in vivo*. However, the composition of the SrBG/PMMA composite cements after implantation was not studied, and hence it was not possible to track the phase transformation of SrBG after implantation. Also, biomechanical tests were not performed, and it cannot be known whether the improved osteointegration of the SrBG/PMMA composite cements in this study may lead to better mechanical stability of the implanted site, or, on the other hand, lead to a compromise of the biomechanical stability of the implanted site owing to uncontrolled degradation. Hence, further *in vivo* study is necessary to investigate the osseointegration of SrBG/PMMA composite cements in an ovariectomized animal model to evaluate treatment in osteoporotic fracture.

5. Conclusion

In this study, bioactive SrBG/PMMA composite cements were developed by adding different amounts of SrBG into PMMA cement as the reinforcement phase and bioactive filler. The SrBG/PMMA composite cements demonstrated proper setting time and high mechanical strength, which complied with the ISO 5833 standard. In addition, the SrBG particles in the composite cements reacted and converted into hydroxyapatite to form an apatite layer on the cement surface after soaking in SBF and PBS, and released ion products (such as Ca, P, B and Sr), imparting bioactivity to the composite cement. When cultured with SrBG/PMMA composite cements, MC3T3-E1 cells showed enhanced vertical migration, proliferation, ALP activity and collagen secretion, confirming the cytocompatibility of the composite cement. Moreover, when implanted in rat tibia defects, SrBG in the composite cements converted into hydroxyapatite and stimulated new-bone formation around the interface between the implants and host bone at eight and 12 weeks post-implantation, whereas pure PMMA bone cement only showed an intervening soft tissue layer, suggesting that the SrBG/PMMA composite cements presented better osseointegration and capacity to regenerate bone defects than PMMA

bone cement. Therefore, the SrBG/PMMA composite bone cements may be a better alternative to PMMA in future clinical applications and is a promising option for bone repair in different defect sites, as it requires minimal invasive surgery.

Ethics. All participants gave informed consent prior to data collection. Cell experiments were supported by Shenzhen Institute of Advanced Technology, Chinese Academy of Sciences. The animal study was approved by Animal Care Committee of Shenzhen Institute of Advanced Technology, Chinese Academy of Sciences.

Data accessibility. The data supporting this article have been registered on Baidu Netdisk and can be accessed via http://pan.baidu.com/disk/home#list/vmode=list&path=%2Frsif-2016-1057.

Authors' contributions. X.C., C.H. and M.Z. carried out the experiments; X.C. and C.R. wrote and revised the paper; S.P., L.L., W.L. and T.W. participated in provision of study material, collection and assembly of data; B.L., W.H., M.N.R. and W.W.L. made substantial contributions to conception and design; C.R. and H.P. gave financial support, revised critically for important intellectual content of this study. All authors gave final approval for publication.

Competing interests. We declare we have no competing interests.

Funding. This work was supported by the National Natural Science Foundation of China (grant nos. 51372170, 51272274), the Development of Strategic Emerging Industries of Shenzhen Project (grant nos. CXZZ20150401152251209, JSGG20150331154931068), the Shenzhen Peacock Innovation Team (grant no. 110811003586331), the Key International S & T Cooperation (grant no. 2015DFH50230) and the Youth Talents of Guangdong Science and Technology Innovation (grant no. 2015TQ01X076).

Acknowledgements. The authors thank Yin Zhao (Shenzhen Institute of Advanced Technology, Chinese Academy of Sciences) and Ruiran Hao (Institute of Chemistry, Chinese Academy of Sciences) for comments on earlier versions of the manuscript.

References

1. Sharma S, Lammin K, Kay P. 2012 Introduction and follow-up of new implants. *Curr. Orthop.* **26**, 231–236. (doi:10.1016/j.mporth.2012.08.002)
2. Shridhar P, Chen YF, Khalil R, Plakseychuk A, Cho SK, Tillman B, Kumta PN, Chun YJ. 2016 A review of PMMA bone cement and intra-cardiac embolism. *Materials* **9**, 821. (doi:10.3390/ma9100821)
3. Xin L *et al.* 2016 Decreased extrusion of calcium phosphate cement versus high viscosity PMMA cement into spongious bone marrow—an *ex vivo* and *in vivo* study in sheep vertebrae. *Spine J.* **16**, 1468–1477. (doi:10.1016/j.spinee.2016.07.529)
4. Chen L, Zhai D, Huan Z, Ma N, Zhu H, Wu C, Chang J. 2015 Silicate bioceramic/PMMA composite bone cement with distinctive physicochemical and bioactive properties. *RSC Adv.* **5**, 37 314–37 322. (doi:10.1039/C5RA04646G)
5. Zhang CL, Shen GQ, Zhu KP, Liu DX. 2016 Biomechanical effects of morphological variations of the cortical wall at the bone–cement interface. *J. Orthop. Surg. Res.* **11**, 72. (doi:10.1186/s13018-016-0405-y)
6. Lewis G. 1997 Properties of acrylic bone cement: state of the art review. *J. Biomed. Mater. Res.* **38**, 155–182. (doi:10.1002/(SICI)1097-4636(199722)38:2<155::AID-JBM10>3.0.CO;2-C)
7. Shinzato S, Nakamura T, Kokuba T, Kitamura N. 2001 A new bioactive bone cement: effect of glass bead filler content on mechanical and biological properties. *J. Biomed. Mater. Res.* **54**, 491–500. (doi:10.1002/1097-4636(20010315)54:4<491::AID-JBM40>3.0.CO;2-0)
8. Miola M, Fucale G, Maina G, Enrica Verné E. 2017 Composites bone cements with different viscosities loaded with a bioactive and antibacterial glass. *J. Mater. Sci.* **52**, 5133–5146. (doi: 10.1007/s10853-017-0750-1)
9. Arcos D, Ragel CV, Vallet-Regí M. 2000 Bioactivity in glass/PMMA composites used as drug delivery system. *Biomaterials* **22**, 701–708. (doi:10.1016/S0142-9612(00)00233-7)
10. Samad HA, Jaafar M, Othman R, Kawashita M, Razak NHA. 2011 New bioactive glass-ceramic: synthesis and application in PMMA bone cement composites. *Bio-Med. Mater. Eng.* **21**, 247–258. (doi:10.3233/BME-2011-0673)
11. Dalby MJ, Silvio LD, Harper EJ, Bonfield W. 2001 Initial interaction of osteoblasts with the surface of a hydroxyapatite-poly(methylmethacrylate) cement. *Biomaterials* **22**, 1739–1747. (doi:10.1016/S0142-9612(00)00334-3)
12. Fottner A, Nies B, Kitanovic D, Steinbrück A, Mayer-Wagner S, Schröder C, Heinemann A, Pohl U, Jansson V. 2016 Performance of bioactive PMMA-based bone cement under load-bearing conditions: an in vivo evaluation and FE simulation. *J. Mater. Sci. Mater. Med.* **27**, 138. (doi:10.1007/s10856-016-5754-x)
13. Hench LL. 2006 The story of Bioglass®. *J. Mater. Sci. Mater. Med.* **17**, 967–978. (doi:10.1007/s10856-006-0432-z)
14. Rahaman MN, Day DE, Jung SB, Bal BS, Fu Q, Jung SB, Bonewalde LF, Tomsiac AP. 2011 Bioactive glass in tissue engineering. *Acta Biomater.* **7**, 2355–2373. (doi:10.1016/j.actbio.2011.03.016)
15. Jones JR. 2013 Review of bioactive glass: from hench to hybrids. *Acta Biomater.* **9**, 4457–4486. (doi:10.1016/j.actbio.2012.08.023)
16. Jung SB. 2012 Bioactive borate glasses. In *Bioglasses: an introduction* (eds JR Jones, AG Clare), pp. 75–96. New York, NY: Wiley.
17. Cui X *et al.* 2016 An injectable borate bioactive glass cement for bone repair: preparation, bioactivity and setting mechanism. *J. Non-Cryst. Solids* **432**, 150–157. (doi:10.1016/j.jnoncrysol.2015.06.001)
18. Buehler J, Chappuis P, Saffar JL, Tsouderos Y, Vignery A. 2001 Strontium ranelate inhibits bone resorption while maintaining bone formation in alveolar bone in monkeys (Macacafascicularis). *Bone* **29**, 176–179. (doi:10.1016/S8756-3282(01)00484-7)
19. Reginster JY. 2002 Strontium ranelate in osteoporosis. *Curr. Pharm. Des.* **8**, 1907–1916. (doi:10.2174/1381612023393639)
20. Peng SL, Zhou G, Luk KD, Cheung KM, Li Z, Lam WM, Zhou Z, Lu WW. 2009 Strontium promotes osteogenic differentiation of mesenchymal stem cells through the Ras/MAPK signaling pathway. *Cell. Physiol. Biochem.* **23**, 165–174. (doi:10.1159/000204105)
21. Marie P, Felsenberg D, Brandi M. 2011 How strontium ranelate, via opposite effects on bone resorption and formation, prevents osteoporosis. *Osteoporos. Int.* **22**, 1659–1667. (doi:10.1007/s00198-010-1369-0)
22. Lin KL, Xia LG, Li HY, Jiang XQ, Pan HB, Xu YJ, Lu WW, Zhang ZY, Chang J. 2013 Enhanced osteoporotic bone regeneration by strontium-substituted calcium silicate bioactive ceramics. *Biomaterials* **34**, 10 028–10 042. (doi:10.1016/j.biomaterials.2013.09.056)
23. Gomez F, Alfonso M, Luis A, Ignacio R, Carlos F, Pertega S, Candal A. 2010 Strontium ranelate improves implant osseointegration. *Bone* **46**, 1436–1441. (doi:10.1016/j.bone.2010.01.379)
24. Andersen OZ *et al.* 2013 Accelerated bone ingrowth by local delivery of strontium from surface functionalized titanium implants. *Biomaterials* **34**, 5883–5890. (doi:10.1016/j.biomaterials.2013.04.031)
25. ISO 5833. 2002 Implants for surgery—acrylic resin cements.
26. Yao AH, Wang DP, Huang WH, Fu Q, Rahaman MN, Day DE. 2007 In vitro bioactive characteristics of borate-based glasses with controllable degradation behavior. *J. Am. Ceram. Soc.* **90**, 303–306. (doi:10.1111/j.1551-2916.2006.01358.x)
27. Kokubo T, Takadama H. 2006 How useful is SBF in predicting in vivo bone bioactivity? *Biomaterials* **27**, 2907–2915. (doi:10.1016/j.biomaterials.2006.01.017)
28. ISO 10993. 2009 Biological evaluation of medical devices.
29. Wei XJ, Xi TF, Zheng YF, Zhang CQ, Huang WH. 2014 In vitro comparative effect of three novel borate bioglasses on the behaviors of osteoblastic MC3T3-E1 cells. *J. Mater. Sci. Technol.* **30**, 979–983. (doi:10.1016/j.jmst.2014.07.007)

30. Huang WH, Day DE, Kittiratanapiboon K, Rahaman MN. 2006 Kinetics and mechanisms of the conversion of silicate (45S5), borate, and borosilicate glasses to hydroxyapatite in dilute phosphate solutions. *J. Mater. Sci. Mater. Med.* **17**, 583–596. (doi:10.1007/s10856-006-9220-z)
31. Li YW, Leong JC, Lu WW, Luk KD, Cheung KM, Chiu KY, Chow SP. 2000 A novel injectable bioactive bone cement for spinal surgery: a developmental and preclinical study. *J. Biomed. Mater. Res. A* **52**, 164–170. (doi:10.1002/1097-4636(200010)52:1<164::AID-JBM21>3.0.CO;2-R)
32. Klijn RJ, van den Beucken JP, Felix Lanao RP, Veldhuis G, Leeuwenburgh SC, Wolke JGC, Meijer GJ, Jansen JA. 2012 Three different strategies to obtain porous calcium phosphate cements: comparison of performance in a rat skull bone augmentation model. *Tissue Eng. A* **18**, 1171–1182. (doi:10.1089/ten.tea.2011.0444)
33. Gbureck U, Barralet JE, Spatza K, Grover LM, Thull R. 2004 Ionic modification of calcium phosphate cement viscosity. Part I: hypodermic injection and strength improvement of apatite cement. *Biomaterials* **25**, 2187–2195. (doi:10.1016/j.biomaterials.2003.08.066)
34. Fu Q, Saiz E, Rahaman MN, Tomsia AP. 2011 Bioactive glass scaffolds for bone tissue engineering: state of the art and future perspectives. *Mater. Sci. Eng. C* **31**, 1245–1256. (doi:10.1016/j.msec.2011.04.022)
35. Goldstein SA. 1987 The mechanical properties of trabecular bone: dependence on anatomic location and function. *J. Biomech.* **20**, 1055–1061. (doi:10.1016/0021-9290(87)90023-6)
36. Anselme K. 2000 Osteoblast adhesion on biomaterials. *Biomaterials* **21**, 667–681. (doi:10.1016/S0142-9612(99)00242-2)
37. El-Ghannam A, Ducheyne P, Shapiro IM. 1997 Formation of surface reaction products on bioactive glass and their effects on the expression of the osteoblastic phenotype and the deposition of mineralized extracellular matrix. *Biomaterials* **18**, 295–303. (doi:10.1016/S0142-9612(96)00059-2)
38. Rahaman MN, Bal BS, Huang WH. 2014 Review: emerging developments in the use of bioactive glasses for treating infected prosthetic joints. *Mater. Sci. Eng. C* **41**, 224–231. (doi:10.1016/j.msec.2014.04.055)
39. Bauer TW, Schils J. 1999 The pathology of total joint arthroplasty II. Mechanisms of implant failure. *Skeletal Radiol.* **28**, 483–497. (doi:10.1007/s002560050552)
40. Fottner A, Nies B, Kitanovic D, Steinbrück A, Hausdorf J, Mayer-Wagner S, Pohl U, Jansson V. 2015 In vivo evaluation of bioactive PMMA-based bone cement with unchanged mechanical properties in a load-bearing model on rabbits. *J. Biomater. Appl.* **30**, 30–37. (doi:10.1177/0885328215569092)
41. Okada Y, Kawanabe K, Fujita H, Nishio K, Nakamura T. 1999 Repair of segmental bone defects using bioactive bone cement: comparison with PMMA bone cement. *J. Biomed. Mater. Res. A* **3**, 353–359. (doi:10.1002/(SICI)1097-4636(19991205)47:3<353::AID-JBM9>3.0.CO;2-P)